고액공존금속의 성형기술 심포지엄(Ⅲ) pp.15~32

반용융 성형공정에 있어서 액상편석제어를 위한 압축 D/B 및 응용

Compression D/B for Liquid Segregation Control in Semi-Solid Forming Process and Its Application

강 충 길, 정 경 득, 정 홍 규
C.G. Kang, K.D. Jung, H.K. Jung
부산대학교 기계공학부
Pusan National University, School of Mechanical Engineering
Pusan, 609-735, Korea

ABSTRACT

A relationship between stress and stain is very important to design a die to avoid defects of products during semi-solid forming process.Since the liquid will be of eutectic composition in alloys, liquid segregation will result in significant or undesirable situation. The materials used in this experiment are A357, A390, Al2024 alloys that is fabricated by the electro-magnetic stirring process from Pechiney in France. The compression test was performed by induction heating equipment and MTS.

In order to prevent the liquid segregation, these measured temperature would be useful to control of strain rate during compression test. The liquid segregation is controlled as change of the strain rate and solid fraction during the compression process. The characteristics of flow between solid and liquid phase considering liquid segregation is examined through the above experiments.

In the case of medium and high volume fractions of solid, the distribution of strain rate is calculated by using compression test data of semi-solid materials (SSM). The thixoforming experiments with the designed die are carried out successfully. The die filling patterns of SSM for variation of die temperature and pressing force have been investigated. The hardness of the thixoformed scroll products is evaluated in terms of the microstructure for each position.

Keywords: thixoforming, overflow position, liquid segregation, die temperature, pressing force

1. Introduction

For optimization of net shape forging process with semi-solid materials(SSM), it is important to predict the deformation behavior for variation of strain rate, but the rheological behavior of mushy state alloys is not sufficiently known. Usually, the rheological behaviour of alloys in the semi-solid state has been examined by using parallel plate compression. However, for analysis of the thixoforming process, it should be necessary to conduct a formation of stress-strain curve in semi-solid alloys. In particular, important problem is to prevent segregation of liquid component during deformation. Semi-solid forming is a method to make globular structure, and deformation the nearest desired product in temperature between solidus and liquidus line, and a lot of concerns are focused in several aspects like saving energy and process, etc. [1-2] Since manufacturing technology for semi-solid alloy was discovered in the middle of studying hot tearing phenomena in early 1970's, Suery et al.[4] have studied compression behavior of Sn-15%Pb alloy in semi-solid state and effect of strain rate, and Toyosima et al.[5] have studied simple compression, filtering, and rolling process. They formulate them, applying compressive visco-plastic models for the solid region of materials and Darcy's flow for the liquid region. Kang et al.[6] compared experimental data with results of finite-element analysis for compressing process of semi-solid aluminum(A356) materials using a yield condition for porous material. Kenny et al.[7] reported the best quality production was obtained in the case of SSM forging, at solid fraction of a billet , 60~70 %. Yoshida et al.[8] reported microstructure and liquid flow state with Al-Cu alloy in semi-solid forging. As a result of casting with rapid velocity, using materials of which solid fraction is 60%, it was observed that there is no segregation in the produced specimen. To prevent a segregation of liquid, in forging process, die should be preheated. It is reported that lowest temperature in die reheating, changes in dependant on billet temperature and compressing die shape, and it was reported that the optimal die temperature is 250 to 300℃. Chen[9] reported the experimental deformation behavior, dividing it into deformation behavior of the liquid region according to mutual contact of the liquid region and solid grains, plastic deformation of the solid grains, and contact of the solid grain, in deformation behavior of SSM.

The curve of stress-strain rate of semi-solid material is different from the hot compression phenomenon of established materials for deformation of solid grains in compression forming. It is very important to note that the limiting strain rate does not

increase, but decreases, in accordance with the increase of stress in compression experiments for the utilization of semi-solid forging process. Therefore, in this study, compression experiments have been performed to investigate deformation behavior of semi-solid material with variation of processing parameters such as compression velocity and the solid fraction. In order to produce components without defects, the condition of forging is controlled to increase of stress with increase of strain rate in initial forming process at constant velocity. Therefore the relationship of the velocity variation to the continuous increase of stress with increase of strain rate has been proposed in the compression experiments. The experiments to fabricate scroll products for variation of die temperature, pressure, and pressing holding time were performed. Scroll products fabricated by using semi-solid aluminum alloys were compared in terms of hardness, and the possibility used for the scroll products was examined. Furthermore, the mechanical properties were investigated by testing the hardness of the fabricated scroll products

2. Compression Experiments

The material used in these experiments are ALTHIX(A357, A390) material, which is fabricated by electro-magnetic stirring process, from Pechiney and is Al2024, which is fabricated by hot extrusion in compression ratio 9.37. The chemical composition of each material is shown Table 1. In forming process of semi-solid material, compression experiments have been performed to investigate the relationship of flow character with variation of solid fraction and die velocity. The compression test of semi-solid material is performed with specimen of h=15×20mm at the temperature of 1200℃ of desired solid fraction using an MTS(Material Test System) with an associated electronic furnace. Fig.1 is the schematic diagram of the experimental apparatus used for the compression of the semi-solid aluminum alloy. Temperature, solid fraction, load, displacement and compression velocity are measured during SSM compression test. At first, the stress-strain are investigated from load and displacement. Generally, in SSM compression test, stress decreases from maximum strain. Then the velocity changes at the displacement correspondent to maximum stress, in order to prevent of liquid segregation. In this obtained stress-strain curve, stress increases according to strain increase. Compression experiments have been performed using A357, A390, Al2024 with compression experiment method of A356. For experiment conditions, solid fractions are 50%(620℃), 70%(599℃) and 90%(556℃), and die velocities are 500mm s^{-1}, 200mm s^{-1},

100mm s^{-1}, 10mm s^{-1}, 1mm s^{-1} in the case of Al2024

3. Compression Experiment Results and Discussion

Compression experiments have been performed using A357, A390 and Al2024. Fig.2(a)~(e) show the shape of the specimen at state of 50%(620℃) solid fraction according to change of Vdie =500, 200, 100, 10, 1 mm s-1. we know that surface of specimen proceeds fracture with increase of die velocity. Fig. 3(a)~(e) show the shape of the specimen at state of 70%(599℃) solid fraction according to the change of die velocity. There is small change compared with fs(solid fraction)=50%, but fracture degree of surface is smaller than fs=50%. Fig. 4 (a),(b) show the shape of the specimen at state of 90%(556℃) solid fraction. The barrel was observed like hot compression with increase of solid fraction. Fig. 5~7 show curve of true stress-strain rate according to change of die velocity when the solid fractions are fs=50%, 70%, and 90%. As shown in Fig. 5~Fig. 6, initial stress peak point is observed at strain rate 0.05~0.1. However, from strain of =0.1, stress decreases remarkably and reaches plateau. This phenomenon accounts for by liquid flow being activated and transfer to the free surface area at the specific strain rate, even though the stress increases for densification of the structure and stimulation of liquid flow from the first moment. In compression forming of semi-solid materials on high temperature, surface of specimen was broken away during compression by liquid flow towards surface of the specimen. Therefore, forming method of closed forging shape is needed as free surface does not exist. Fig 7 of fs=90% shows the shape of the specimen at the state of solid fraction differing from Fig .5~Fig .6 of fs=50% , fs=70%. The above cause is that because in high temperature. globularness hasn' t been made in the solid fraction, in the direction of extrusion, orientation of structure doesn't only exist but also liquid flow does not exist, in the first stage of deformation. the stress increases extremely, and as globular microstructure is fracture, stress decreases extremely. Fig. 8 shows that the relationship of stress-strain rate represents that of algebraic coordinates($\log \dot{\varepsilon}$ -$\log \sigma$) using the result of compression experiments with various alloys and temperatue, employing the definition of the coefficients K and m (flow stress equation: $\sigma = K \dot{\varepsilon}^{m}$). The K and m values are solved with linear recursion using a divided interval, as shown in Fig. 8 and Table 2. Fig. 9(a) and (b) show a structural photograph of specimen center and surface compressed with variation of die velocity in the case of fs=50%. When die velocity is

over Vd=100mm s-1, solid grain and liquid phase flow simultaneously, so solid grain is relatively homogeneous in entire cross section. The compression deformation was observed in the middle part of the material by the stick of solid grains and structure size was relatively minute. Fig.10(a)~(c) show flow state of specimen cross-section at height-reduction ration 50%, in case die velocities, Vd are 500mm s^{-1}, 100mm s^{-1}, 1mm s^{-1}. When die velocity, Vd was 500mm s^{-1} as shown in Fig.10(a), the separation phenomenon of solid and liquid phase wasn't observed, but in the case of die velocity was Vd =1mm s^{-1} as shown in fig.10(c) separation phenomenon of solid and liquid phase was made, so after deformation, boundary including porosity was observed and liquid distribution is much around surface. Fig.11 shows the relationship between true strain and stress for variation of strain rate with A357 in case of solid fraction, 50%. In high strain rate of $5.88\times10^{-1}sec^{-1}$, true strain to obtain of maximum stress is 0.1. However, in the case of strain rate less than 29.4 sec^{-1}, maximum stress obtained at the true strain of 0.15. The decreasing rate of stress decreases remarkably from maximum stress when the strain rate increases, as shown in Fig. 5, 6. Fig. 12, 13, is the relationship between true stress and true strain of strain-rate jump at the maximum stress point with A357. The effect of strain-rate jump to prevent liquid segregation is shown in Fig. 14. The macrostructure of the cross-section after compression in semi-solid state shows that the free surface of specimen is maintained when the strain-rate velocity changes and porosity is reduced.

Fig. 15 shows the curve of strain-stress of A390 alloy. The maximum stress except for strain rate, $5.88\times10^{-1}sec^{-1}$ is obtained at true strain of 0.15. In forming process of SSM, the strain rate should be controlled to continuously increase the stress according to increase of strain rate at the position which is shown at a peak point of stress, as shown in Fig. 5, 6, 11 and 15. For understanding this phenomenon, the continuously increase of stress according to increase of strain rate is investigated in compression test. Fig.16 is the curve of stress-strain rate with various compression velocities at a strain, ε =0.1. As shown in Fig.16, the stress increases continuously for the value that strain rate of , 5.88×10^{-2} , 5.88×10^{-1}, 2.353 and 7.058 sec^{-1} are to increase of 5.88×10^{-1}, 2.353, 7.085 and 29.4 sec^{-1} respectively. When compression velocity changes, discontinuity point is found at strain, 0.17. The sharply decrease of stress is considered as an error of time needed to control velocity with high die speed change in Material Testing System. Fig.17 shows jumping strain rate values to obtain continuously increasing strain-stress curve. When initial strain is 5.88×10^{-2} sec^{-1} , and first and

second jump strain rate is 5.88×10^{-1} and 5.88 sec^{-1} respectively. As shown in Fig.16, the data error at the jumping point is also considered because of sensitivity of MTS due to velocity change.

In Fig. 18, the microstructure of A390 after compression shows the effect of strain-rate jump. Because of its chemical composition A390 alloy have less deformation resistance, 1 step strain-rate jump shows enough homogeneous microstructure without porosity compared to 2 step strain-rate jump as shown in Fig. 18.

According to the above experiment , forming limitation will be improved because the lower solid fraction is, the lower load is. It is known that distribution of solid and liquid phase is homogeneous because of distinguished from boundary of Vd=100mm/s as shown in Fig.10(a)~(c)

4. Experiments of 86S Scroll Component

4.1. The method of experiments

Wear resistance test was performed with aluminum alloys (A356, A357, A390, ALTHIX 86S) fabricated by Pechiney in France and cast iron materials used for conventional scroll products. From the results of the test, aluminum material with high applicability was selected, and the thixoforging experiments were performed using this aluminum material. The chemical composition of ALTHIX 86S material used for the thixoforging experiments was shown in Table 1. Fig. 19 shows the relationship between pressing force and die temperature to obtain better products in forming processes of scroll products. It shows possible region for forming and is classified into complete filling (●), non-filling (■) and partial filling (▲). Generally, the higher pressing is at die temperature 200~300℃, the better filling is. Fig. 23 is the photos of scroll component with various filling type. Fig. 20 shows cross-sectional areas of scrolls where the hardness was measured. 5 regions from [A]~[E] were selected for micro vickers hardness test.

4.2. The results of experiments and discussion

For the thixoforging process both the coexisting solidus-liquidus phase, the reheating conditions to obtain the globular microstructure are very important. Jung et al. [10] proposed that the eutectic must be melted completely at over 572℃ (completely eutectic melting temperature of ALTHIX 86S alloy), and the reheating time for the complete eutectic melting is necessary to obtain a fine globular microstructure. So, in this study,

these experimental reports were used. The scroll products with ALTHIX 86S alloy were fabricated with various experimental conditions, and the hardness was measured in [A]~[E] of Fig. 20 and the results of the hardness test were shown in Figs. 21 (a), (b) and (c). Figs. 21 (a), (b), and (c) show the results of the hardness test on the scroll specimen fabricated at the forming conditions of Exp. No.2, No.7 and 8, as shown in Table 3. As shown in Figs. 21 (a) and (b), the hardness is 75~85Hv at the Exp. No.2 and 8 but at the Exp. No.7, the hardness is 55~60 Hv in [A]~[D], and low relatively. The above reason is that filling looks good apparently but as cooling rate affecting on the grain size reduces, the globular microstructure is not created but dendrite. Fig. 22 is the photos of 86S scroll component with various filling type. Semi-solid material (SSM) properties have a great influence on the local strain rate, solid fraction, and processing technology. As SSM is filled into the die cavity, the material is not uniformly strained throughout. This results in both temporal and spatially-varying strains and strain rates. To analyze thoroughly a die filling and improve the mechanical properties of thixoformed products, all of these factors properly accounted for in the material model. Defects of products occurring during thixoforming are unfilling phenomena in the die filling, oxide films, segregation of eutectic, coarsening of Si particles, shrinkage pores and so on. From the above results, thixoforming technology proposed in this study would result in the reduction of lead-time and promotion of the thixoforming technology.

5. Conclusions

In the compression test of semi-solid aluminum materials, the following results were obtained from investigation of the deformation and the transformation of the macrostructure, considering the strain rate.

(1) From the macrostructure change appearing in the compression behavior of SSM, more homogeneous structure phenomena can be observed with greater compressive velocity.

(2) In the compression tests of SSM, macro-separation appeared between the solid and the liquid region because of the outflow of the liquid state, densification of the structure was observed in the middle of part, and less porosity is outflow to the surface was observed, with a greater compressive velocity.

(3) After compressing forming of Al2024 material, the faster deformation rate was, the more distribution of solid and liquid phase was homogeneous and critical rate to

distribute solid and liquid phase homogeneously, was about Vd=100mm s^{-1}.

(4) From compressing experimental result using A357, A390 and Al2024, database of semi-solid materials can be obtained to prevention of liquid segregation, in compressing forming process, through change of strain rate, the method of compression experiments by control of solid fraction and liquid phase was suggested.

(5) Through the compression experiment results, fabrication of high quality scroll component without liquid segregation was successfully conducted

6. Acknowledgements

This work has been supported by the Engineering Research Center for Net Shape and Die Manufacturing (ERC/NSDM) of Pusan National University which is financed jointly by Korean Science and Engineering Foundation(KOSEF)

7. References

1. C.G. Kang, J.S. Choi ,D.W. Kang,1998. A Filling Analysis of the Forging Process of Semi-Solid Aluminum Materials Considering Solidification Phenomena. J. Materials Processing technology, 73, 289-302.
2. M.C. Flemings, 1991. Behavior of Metal Alloys in the Semi-Solid State. Metallurgical Transaction, 27A, 957-981.
3. D.B. Spencer, R. Merabian and M.C. Flemings,1972. Rheology of Semi-Solid Dendritic Sn-Pb Alloys at Low Strain Rates, Metall. Trans., 3, 1925-1932.
4. M. Suery and M.C. Flemings, 1982. Effect of Strain Rate on Deformation Behavior of Semi-Solid Dendritic Alloys, Metall. Trans., 13(A),1809-1819.
5. S. Toyoshima, 1994. A FEM Simulation of Densification in Forming Processes for Semi-Solid Materials Processings of the 3rd Int. Conf., on Processing of Semi-Solid Alloys and Composites, University of Tokyo, 47-62.
6. C.G. Kang, B.S. Kang, and J.L Kim, 1998. An Iinvestigation of the Mushy State Forging Process by the Finite Element Method. Journal of Materials Processing Technology,80(81),444-449
7. M.P. Kenny, J.A. Courtois, R.D. Evans, G.M.Farrior, C.P. Kyonka, A.A. Couch, K.P. Young Semi-Solid Metal Casting and Forming, Metal Handbook, 9th Ed., 15, 327-338.

8. C. Yoshida, M. Moritaka, S. Shinya, S. Yahata, K. Takebayashi, A. Nanba,1992. "Semi-Solid Forging
Aluminium Alloy", 2nd Int. Conf., on the Processing of Semi-Solid Alloys and Composites MIT, 95-102.
9. C.P. Chen, X-Ya Tsao, 1996. Semi-solid deformation of A356 Al alloys. Proceedings of the fourth International Conference on Semi-solid Processing of Alloys and Composites, 16-20.
10. H.K. Jung & C.G. Kang, 1999, An Induction Heating Process with Coil Design and Solutions Avoiding Coarsening Phenomena of Al-6%Si-3%Cu-0.3%Mg Alloy for Thixoforming. Metalurgical. & Materials Transactions A, Vol.30A, No.12, pp. 1-11.

Table 1. Chemical composition of A357(ALTHIX), Al2024, A390(ALTHIX) and 86S(ALTHIX)

		Si	Fe	Cu	Mn	Mg	Cr	Zn	Ti	Pb
A357	Min(%)	6.5	-	-	-	0.30	-	-	-	-
	Max(%)	7.5	0.15	0.03	0.03	0.40	-	0.05	0.20	0.03
Al2024	Min(%)	-	-	3.8	0.3	1.2	-	-	-	-
	Max(%)	0.50	0.70	4.9	0.9	1.8	0.10	0.25	0.15	-
A390	Min(%)	16.0	-	4.0	-	0.5	-	-	-	-
	Max(%)	17.0	0.4	5.0	0.1	0.65	-	0.05	0.2	0.03
86S	Min(%)	5.5	-	2.5	-	0.30	-	-	-	-
	Max(%)	6.5	0.15	3.5	0.03	0.40	-	0.05	0.20	0.03

Table 2. K and m values with various alloys and temperature as shown in Fig. 8

alloy	A356			A357		A390	86S		Al2024	
symbol	+		×	■	◆	●	▲	■	□	○
Temp.℃	584		572	585	565	567	577	563	620	599
K	1.02	0.29	12.61	0.65	3.43	0.34	0.32	1.57	0.494	1.336
m	0.32	0.7	0.29	0.52	0.37	0.48	0.43	0.37	0.209	0.476

Table 3. Scroll forming condition by using ALTHIX 86S alloy with d×l=76×30(mm) in thixoforming process

Exp. No.	Die Temperature Td (℃)	Pressing Force P (MPa)	Pressing Holding Time tp (sec)
2	200	104	20
7	250	80	45
8	250	80	20

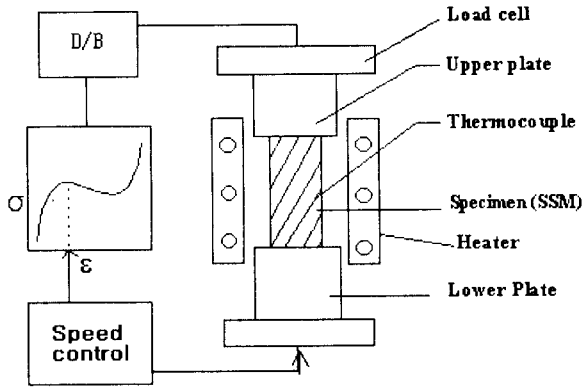

Fig. 1. Schematic diagram of intelligent compression test to prevention of liquid segregation during experiment of SSM

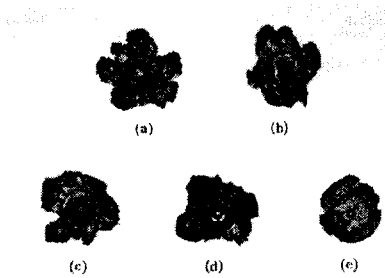

Fig. 2. Specimen after compression at fs=50% (Al2024)
(a) Vd = 500mm/sec (b) Vd = 200mm/sec (c) Vd = 100mm/sec
(d) Vd = 10mm/sec (e) Vd = 1mm/sec

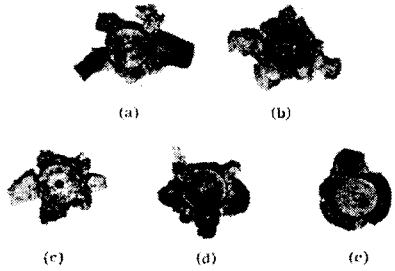

Fig. 3. Specimen after compression at fs=70% (Al2024)
(a)Vd = 100mm/sec (b)Vd = 200mm/sec (c)Vd = 100mm/sec
(d)Vd = 10mm/sec (e)Vd = 1mm/sec

Fig. 4. Specimen after compression at fs=90%(Al2024)
(a)Vd = 10mm/sec (b)Vd = 1mm/sec

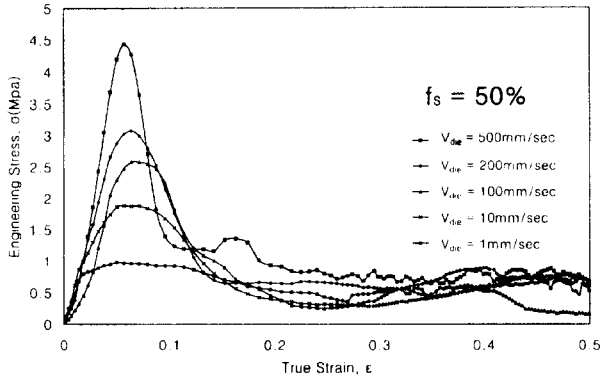

Fig. 5. Engineering stress-true strain Curve at fs=50%
(Al2024)(Vd= 500mm/sec~1mm/sec)

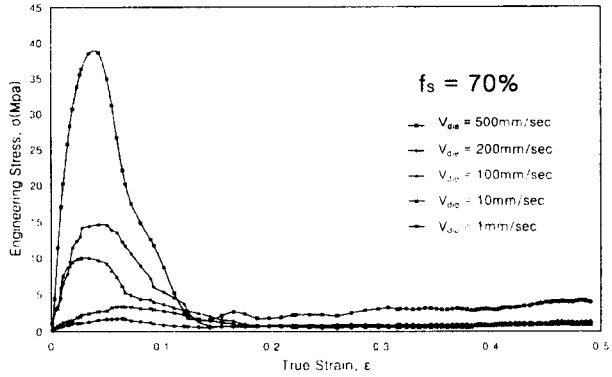

Fig. 6. Engineering stress-true strain curve at fs=70% (Vd= 500 mm/sec ~ 1 mm/sec)

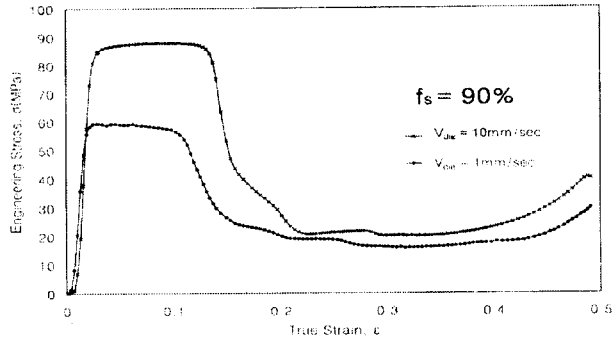

Fig. 7. Engineering stress-true strain curve obtained at fs=90% (Al2024)(Vd = 10mm/sec ~ 1mm/sec)

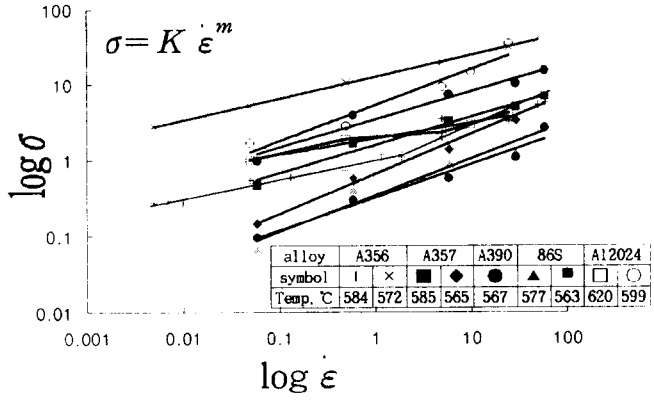

Fig. 8. Relationship between log $\dot{\varepsilon}$ and log σ with various alloys and temperature

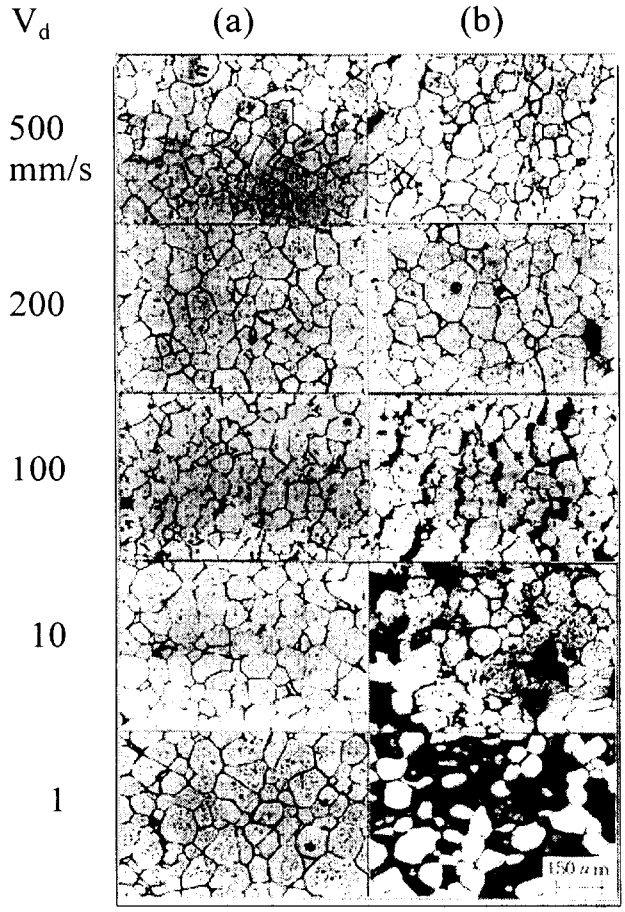

Fig. 9. Evolution of the microstructure of semi-solid alloy upsetting for variation of die speed(fs=50%, 620℃)

(a) Vd=500mm/sec (b) Vd=100mm/sec (c) Vd=1mm/sec

Fig. 10. The microscopic photo of cross-section compressed at solid fraction fS=50%, reduction ratio of 50%

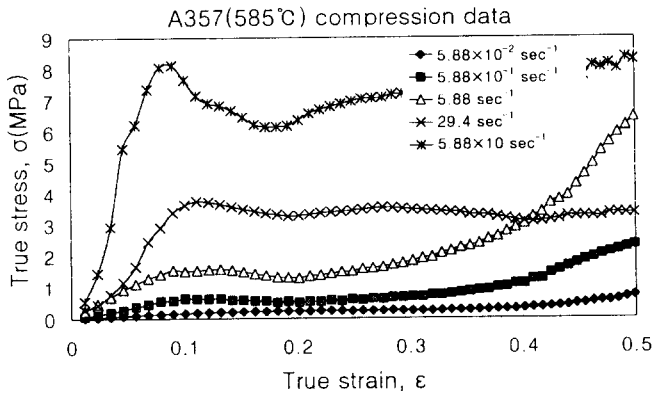

Fig. 11. Engineering stress-true strain curve (A357) for variation of strain rate at fs=50%

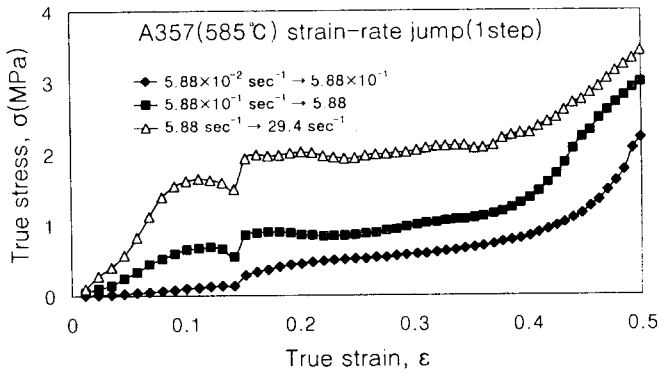

Fig. 12. Engineering stress-strain curve obtained for variation of each initial compression velocity to prevention of liquid segregation(A357)

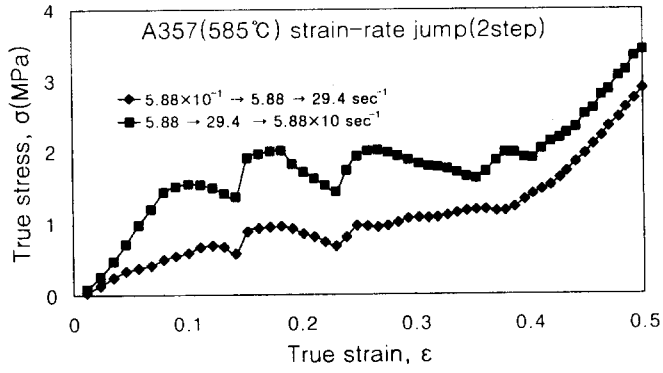

Fig. 13. Engineering stress-strain curve obtained for variation of each initial compression velocity to prevention of liquid segregation(A357)

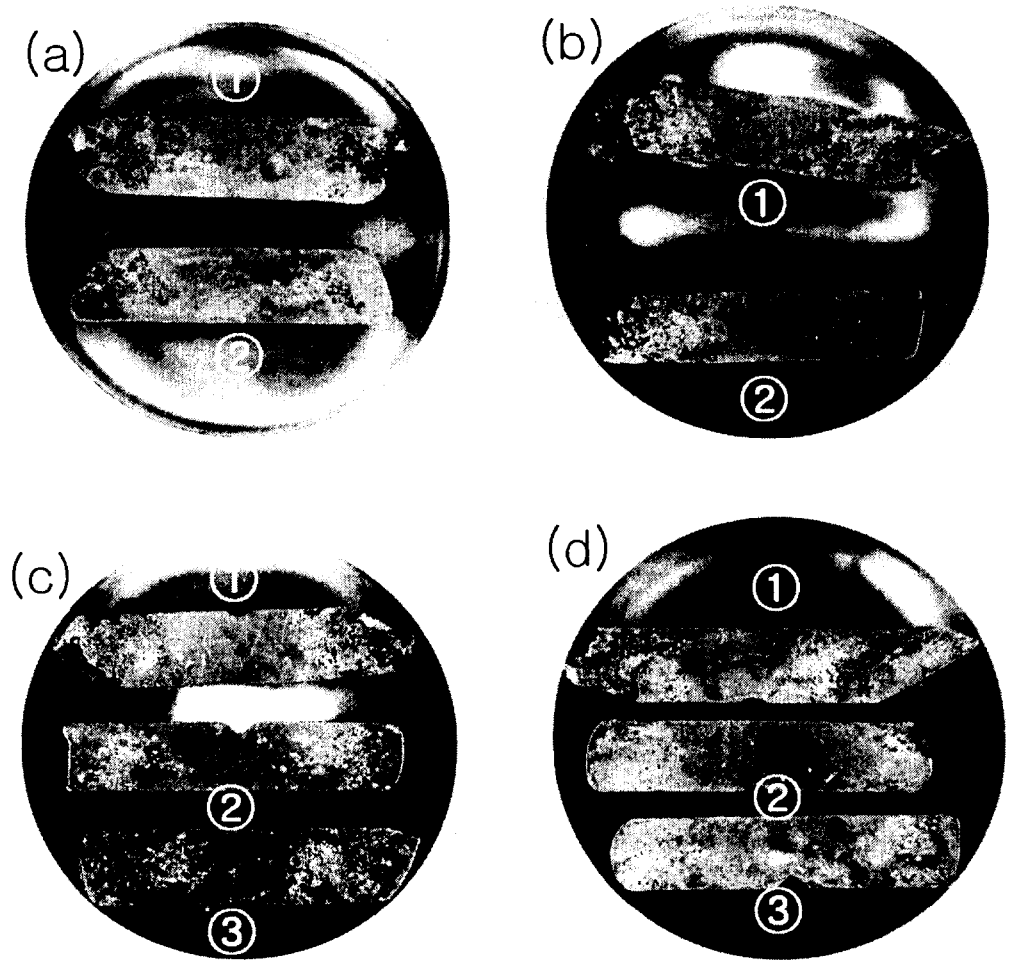

Fig. 14. Macrostructure of A357 compression specimen with constant strain rate and variation of strain rate at decreasing point of stress(585℃)

(a) ①:5.88×10^{-1} sec^{-1}, ②:5.88×10^{-2} → 5.88×10^{-1} sec^{-1}

(b) ①:5.88×10 sec^{-1}, ②:5.88 → 29.4 → 5.88×10 sec^{-1}

(c) ①:5.88 sec^{-1}, ②:5.88×10^{-1}→5.88 sec^{-1}, ③ 5.88×10^{-2}→5.88×10^{-1}→5.88 sec^{-1}

(d) ①:29.4 sec^{-1}, ②:5.88→29.4 sec^{-1}, ③ 5.88×10^{-1}→5.88→29.4 sec^{-1}

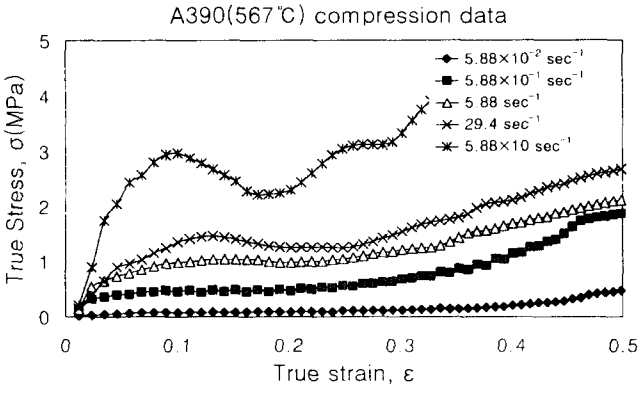

Fig. 15. Engineering stress-true strain curve (A357) for variation of strain rate at fs=50%

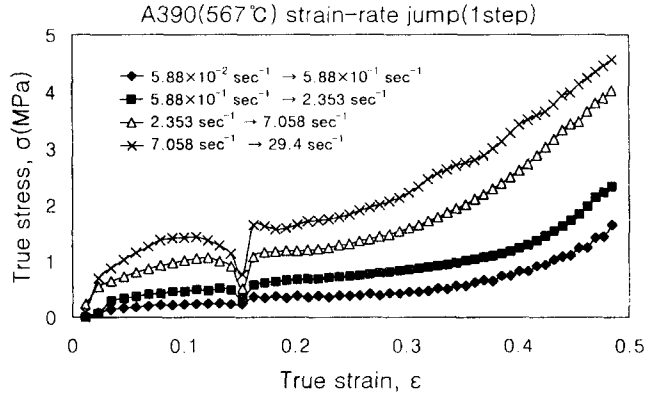

Fig. 16. Engineering stress-strain curve obtained for variation of each initial compression velocity to prevention of liquid segregation(A390)

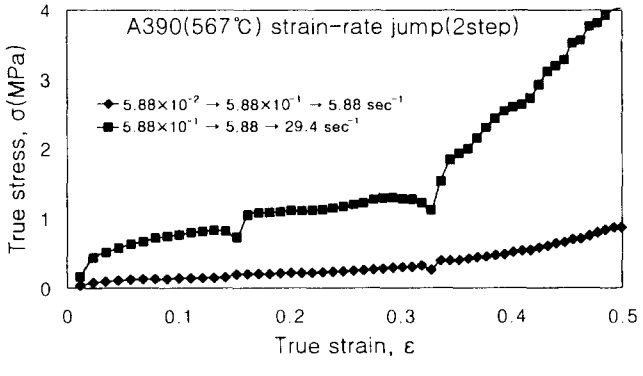

Fig. 17. Engineering stress-strain curve obtained for variation of each initial compression velocity to prevention of liquid segregation(A390)

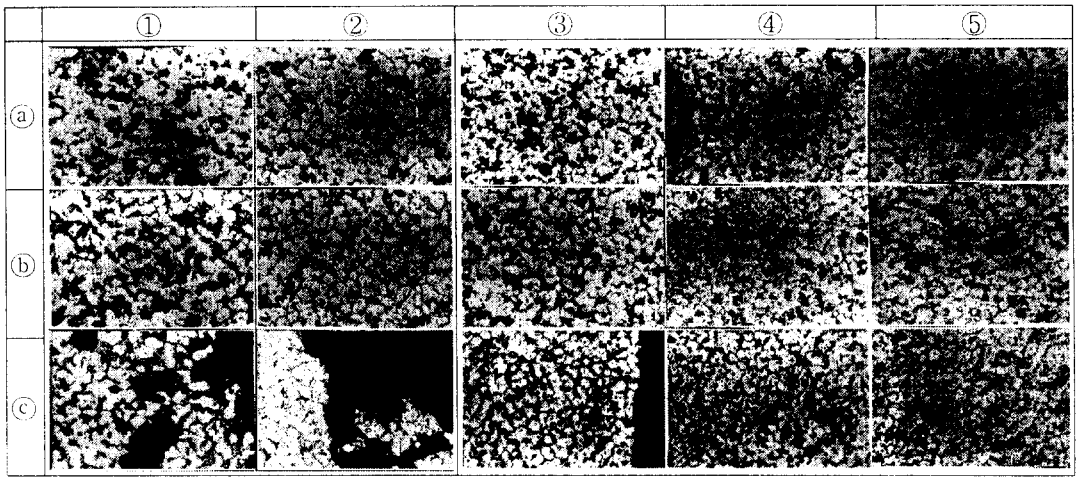

Fig. 18. Microstructure of A390 compression specimen with constant strain rate and variation of strain rate at decreasing point of stress(567℃)

① : 5.88×10^{-1} sec^{-1}

② : 29.4 sec^{-1}

③ : 5.88×10^{-2} → 5.88×10^{-1} sec^{-1}

④ : 7.05 → 29.4 sec^{-1}

⑤ : 5.88×10^{-1} → 5.88 → 29.4 sec^{-1}

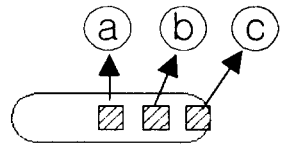

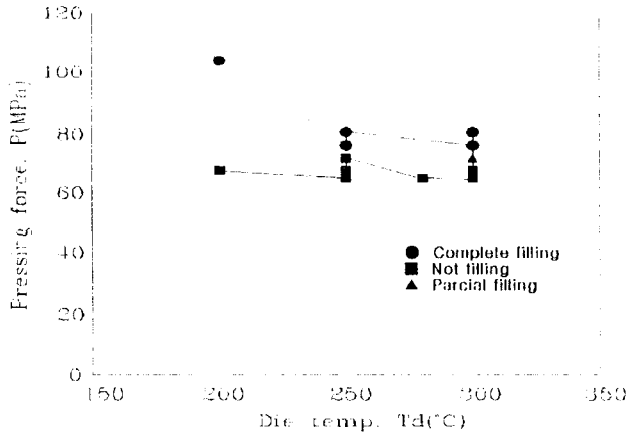

Fig. 19. Relationship between die preheating temperature and pressing force to obtain the good product in fabrication process of scroll components

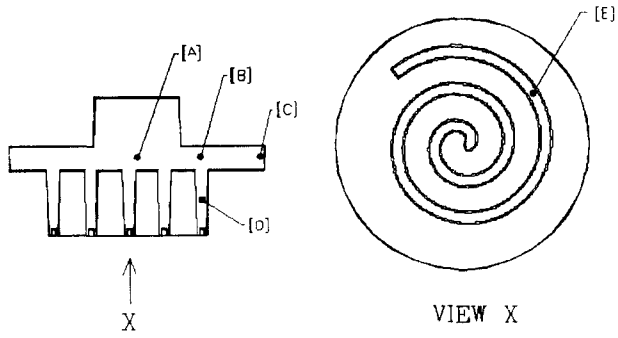

Fig. 20. Positions of scroll product to investigate microstructures

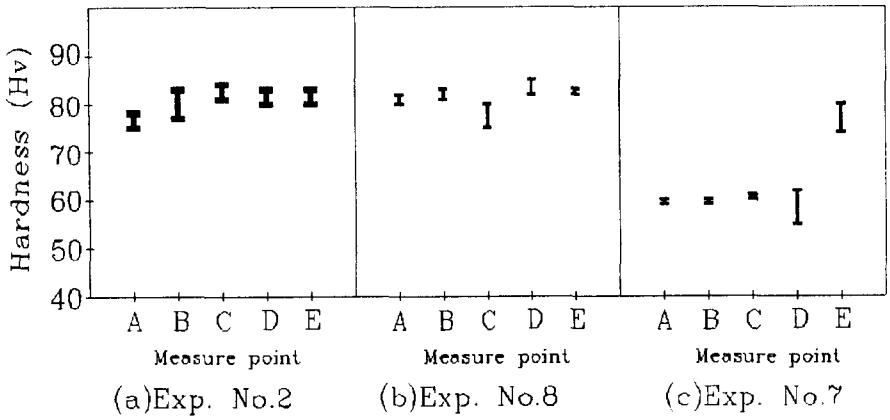

Fig. 21. The Microhardness of 86S products after thixoforging with various conditions

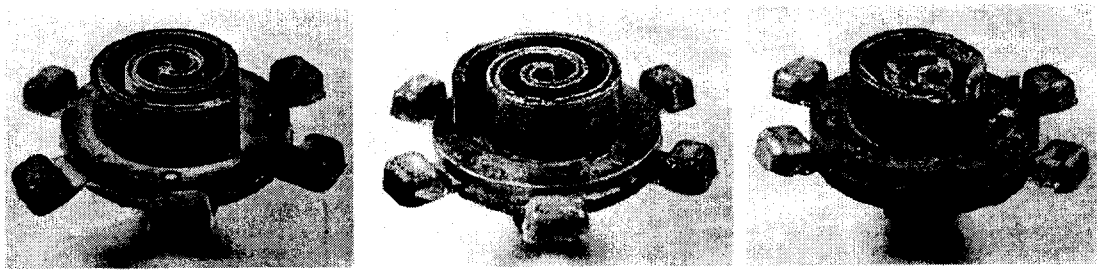

(a) Complete filling (●) (b) Partial filling (▲) (c) Defective filling (■)

Fig. 22. Scroll produced by thixoforming using ALTHIX 86S aluminum alloy